



Environmentally Relevant Supramolecular Metal Coordination Polymers Derived from 5-(3-Pyridyl)-1,3,4-Oxadiazole-2-Thiole and Imidazole

AREF A.M. ALY*, MAHMOUD A. GHANDOUR,
BAHAA M. ABU-ZIED and MAGED S. AL-FAKEH

Department of Chemistry, Faculty of Science, Assiut University, Assiut Egypt.

*Corresponding author E-mail: maged7969@yahoo.com

(Received: December 25, 2012; Accepted: January 16, 2013)

ABSTRACT

A number of supramolecular coordination polymers of cobalt (II), nickel (II), copper (II), cadmium (II) and lead (II), 5-(3-pyridyl)-1,3,4-oxadiazole-2-thiol (POZT) and imidazole (IMZ) has been prepared and characterized. The compounds have been characterized based on elemental analysis, FT-IR and electronic spectral studies and thermal analysis. Thermogravimetry (TG), derivative thermogravimetry (DTG) and differential thermal analysis (DTA) have been used to study the thermal decomposition steps and to calculate the thermodynamic parameters of the metal coordination polymers. The kinetic parameters have been calculated from the Coats-Redfern and Horowitz-Metzger equations. The antimicrobial activity of the synthesized compounds was tested against six fungal and five bacterial strains. The majority of compounds were effective against the tested microbes. The bacteria and fungi strains are common contaminants of the environment in Egypt e.g. some of which are frequently reported from contaminated soil, water and food, or involved in human and animal diseases.

Key words: Coordination polymers, FT-IR, thermal studies and biological activity.

INTRODUCTION

Currently, the construction of metal-organic coordination architectures has witnessed tremendous growth because of their intriguing structures, gas storage and potential properties¹⁻⁴. Among heterocyclic thioamides bearing the $-N(H)-C(=S)-$ or $-N=C(-SH)-$ group,⁵ an oxadiazole functional derivative 5-(3-pyridyl)-1,3,4-oxadiazole-2-thiol has been introduced in the design of new porous coordination polymers very recently⁶. At the same time, it has been found that the geometry of

metal ion is responsible for structural diversification of such MOFs as well as the synthetic route⁶. A pyridyl-type group that is able to satisfactorily complete the coordination sphere of the metal center usually leads to the formation of novel coordination polymers⁷. It has a strong capability of forming hydrogen bonding interactions that play an important role in the assembly of supramolecular compounds. The imidazole ring is present in many biological systems (nucleic acid, proteins, antibiotics, therapeutic agents and cofactors) and plays a significant role in acid or base chemistry,

catalysis, H-bonding and metal complexation⁸. The ligation properties of these donor groups are widely utilized in biomolecules physiologically planned to interact with metal ions, for instance the imidazole moiety of the histidyle residue in a large number of metalloproteins forms all or part of the binding site of the metal(II) ions⁹⁻¹⁰. Furthermore, thermal analysis methods play an important role in studying the structures and properties of metal coordination polymers. They were applied to determine the thermal stability ranges, the thermal character of the decomposition products. The present work describes the preparation and characterization of some mixed-ligand complexes of cobalt(II), nickel(II), copper(II), cadmium(II) and lead(II) containing POZT and IMZ. Figure 1 shows the structure of the ligands.

EXPERIMENTAL

Materials

High purity 5-(3-pyridyl)-1,3,4-oxadiazole-2-thiol and imidazole were purchased from Sigma Aldrich and Alpha Chemika. All other chemicals were of AR grade.

Synthesis of the coordination polymers

Synthesis of the mixed ligand coordination polymers of 5-(3-pyridyl)-1,3,4-oxadiazole-2-thiol and imidazole with Co(II), Ni(II), Cu(II), Cd(II) and Pb(II) follows essentially the same procedure. $[\text{Co}(\text{POZT})(\text{IMZ})\text{Cl}(\text{H}_2\text{O})_2]_n$ synthesis is typical. An ethanolic solution 10 mL of POZT (0.1 g, 0.5 mmol) was slowly added into a hot ethanolic solution (10 mL) of $\text{CoCl}_2 \cdot 6\text{H}_2\text{O}$ (0.132 g, 0.5 mmol) and to it an ethanolic solution (10 mL) of imidazole (0.038 g, 0.5 mmol) was added dropwise. The resultant mixture was stirred for 1 h and filtered. The Light-blue precipitate was separated, washed with distilled water and EtOH and then dried over CaCl_2 in a desiccator.

Physical measurements

Stoichiometric analysis (carbon, hydrogen, nitrogen and sulphur) were performed using Analytischer Funktionstest Vario El Fab-Nr.11982027 elemental analyzer. Infrared spectra were recorded as KBr disks ($400\text{-}4000\text{ cm}^{-1}$) with a FT-IR spectrophotometer and the electronic spectra were obtained using a Shimadzu UV- 2101 PC spectrophotometer. Magnetic susceptibility measurements were done on a magnetic

susceptibility balance of the type MSB-Auto. The conductance was measured using a conductivity Meter model 4310 JENWAY. Thermal studies were carried out in dynamic air on a Shimadzu DTG 60-H thermal analyzer at a heating rate $10\text{ }^\circ\text{C min}^{-1}$. Scanning electron microscope was of the type JEOL JFC-1100E ION SPUTTERING DEVICE, JEOL JSM-5400LV SEM. SEM specimens were coated with gold to increase the conductivity.

Biological activity

The antimicrobial activity of 1, 4 and 5 were tested against 5 bacterial and 6 fungal strains. All microbial strains were kindly provided by the Assiut University Mycological Centre (AUMC). These strains are common contaminants of the environment in Egypt and some of which are involved in human and animal diseases (*Candida albicans*, *Geotrichum candidum*, *Scopulariopsis brevicaulis*, *Aspergillus flavus*, *T.rubrum*, *Staphylococcus aureus*), plant diseases (*Fusarium oxysporum*) or frequently reported from contaminated soil, water and food substances (*Escherichia coli*, *Bacillus cereus*, *Pseudomonas aeruginosa* and *Serratia marcescens*). To prepare inocula for bioassay, bacterial strains were individually cultured for 48h in 100 ml conical flasks containing 30 ml nutrient broth medium. Fungi were grown for 7 days in 100 ml conicals containing 30 ml Sabouraud's dextrose broth. Bioassay was done in 10 cm sterile plastic Petri plates in which microbial suspension (1ml/plate) and 15 ml appropriate agar medium (15 ml/plate) were poured. Nutrient agar and Sabouraud's dextrose agar were respectively used for bacteria and fungi. After solidification of the media, 5 mm diameter cavities were cut in the solidified agar (4 cavities/plate) using sterile cork borer. The chemical compounds dissolved in dimethyl sulfoxide (DMSO) at 2%w/v (=20 mg/ml) were pipetted in the cavities (20 μl /cavity). Cultures were then incubated at 28°C for 48 h in case of bacteria and up to 7 days in case of fungi. Results were read as the diameter (in mm) of inhibition zone around cavities (see Kwion- Chung and Bennett, 1992).

RESULTS AND DISCUSSION

The coordination polymers were prepared by the reaction of 5-(3-pyridyl)-1,3,4-oxadiazole-2-thiol (neutralized with NaOH), metal chlorides or

nitrate, and imidazole (dissolved in EtOH). The prepared compounds were found to react in the molar ratio 1: 1: 1 metal: POZT: IMZ. The coordination polymers are air stable, insoluble in common organic solvents but partially soluble in DMSO. The electrical conductivity of the complexes indicate that they are of non-electrolyte nature¹¹. The compositions of the compounds are supported by the elemental analysis recorded in Table (1) together with color, melting points and conductivity of the coordination polymers.

Fourier transforms infrared spectroscopy (FT-IR)

The IR spectra of the coordination polymers can be seen in Table (2). The bands observed in the 1598-1608 cm⁻¹ regions are assigned to the $\nu(\text{C}=\text{N})$ stretching vibration of the POZT¹². IMZ exhibits in the complexes a band in the region 814-825 cm⁻¹ which can be assigned to $\nu(\text{C}-\text{N})$. This band is positive shifted if compared with that of the free imidazole at 840 cm⁻¹.¹³ Observation of a band in the region 3096-3144 cm⁻¹ indicates the existence of $\nu(\text{N}-\text{H})$ of the IMZ ligand¹⁴. Furthermore, it is found that the bands at 3357-3390 cm⁻¹ in the spectra of 1, 2, 4 and 5 compounds are assigned to νOH of coordinated water¹⁵, whereas the νOH stretching vibrations of the crystallization water molecules are located at 3260 and 3270 cm⁻¹ for compounds 2 and 5.¹⁶ Metal-oxygen and metal-nitrogen bonding are manifested by the appearance of a band in the 504-542 cm⁻¹ and 418-442 cm⁻¹ regions, respectively¹⁷. (Fig.2).

Electronic Spectra

The electronic spectra of the compounds in dimethylsulphoxide (DMSO) display two absorption maxima located in the regions 37,037-38,759 and 28,571-32,679 cm⁻¹ which are attributed respectively to $\pi \rightarrow \pi^*$ and $n \rightarrow \pi^*$ transitions within the POZT and IMZ ligands^{12,18}. The Co(II), Ni(II) and Cu(II) coordination polymers exhibit respectively a band at 19,569, 20,120 and 19,047 cm⁻¹ corresponding to the d-d transitions. Additionally, the magnetic moments of the compounds were measured and it has been found that the Co(II) compound 1 has a magnetic moment of 4.38 B.M typical of the octahedral complexes¹⁹ whereas the magnetic moment values 3.08, 2.05 B.M was found

Table 1: Physical properties and elemental analysis of the compounds

Compound	M. F (M.Wt)	Color	Found (Calcd. %)			m.p.°C (Decom.)	Λ_m Scm ² mol ⁻¹
			C	H	N		
1	[Co(POZT)(IMZ)Cl(H ₂ O) ₂] _n CoC ₁₀ H ₁₂ N ₅ SO ₃ Cl (376.72)	Light-Blue	32.10 31.88	3.72 3.21	17.50 18.59	275	13.25
2	[Ni(POZT)(IMZ)Cl(H ₂ O) ₂] _n NiC ₁₀ H ₁₂ N ₅ SO ₃ Cl (376.48)	Light-Green	31.91 31.90	4.11 3.21	17.57 18.60	266	15.50
3	{[Cu(POZT)(IMZ)Cl]·H ₂ O} _n CuC ₁₀ H ₁₀ N ₅ SO ₂ Cl (363.32)	Brown	32.91 33.05	3.44 2.77	18.72 19.28	282	11.82
4	[Cd(POZT)(IMZ)Cl(H ₂ O) ₂] _n CdC ₁₀ H ₁₂ N ₅ SO ₃ Cl (430.19)	White	28.10 27.91	3.02 2.81	15.01 16.28	273	12.24
5	{[Pb(POZT)(IMZ)(NO ₃)(H ₂ O) ₂]·4H ₂ O} _n PbC ₁₀ H ₂₀ N ₆ SO ₁₀ (623.63)	White	20.33 19.25	3.27 3.23	12.06 13.47	258	10.12

for the Ni(II) 2 and Cu(II) 3 compounds respectively indicating their octahedral and tetrahedral structures, respectively²⁰⁻²¹. An octahedral structure was supposed for Cd(II) 4 and Pb(II) 5 compounds.

The electronic spectral data are shown in Table (3). From the foregoing data the structure of the compounds can be postulated as follows (Fig.3).

Table 2: Infrared Spectral Data of the Compounds

Compounds	$\nu(\text{H}_2\text{O})$	$\nu(\text{N-H})$	$\nu(\text{C-N})$	$\nu(\text{C=N})$	$\nu(\text{M-N})$	$\nu(\text{M-O})$
1	3357	3110	815	1607	430	542
2	3384	3115	814	1608	438	540
3	3260	3096	822	1598	442	504
4	3390	3144	825	1600	428	524
5	3498,3270	3100	818	1602	418	533

Table 3: Electronic spectral data and magnetic moments of the compounds

Compound	ν_{max} (cm ⁻¹)	Assignment	μ_{eff} B.M
1	19,569	d-d transition	4.38
	31,250	n→ π^* transition	
	38,167	π → π^* transition	
2	20,120	d-d transition	3.08
	28,571	n→ π^* transition	
	37,313	π → π^* transition	
3	19,047	d-d transition	2.05
	28,089	n→ π^* transition	
	37,037	π → π^* transition	
4	31,847	n→ π^* transition	-
	37,593	π → π^* transition	
5	32,679	n→ π^* transition	-
	38,759	π → π^* transition	

Table 4: Thermal decomposition data of the compounds in dynamic air

Compound	Step	TG/DTG			Mass Loss(%)
		Ti	Tm	Tf	
2	1 st	50	158	178	8.53
	2 nd	180	315	370	33.16
	3 rd	372	406	453	19.03
	4 th	455	520	750	18.65
3	1 st	120	194	260	5.70
	2 nd	261	374	391	53.44
	3 rd	392	413	443	7.88
	4 th	445	660	750	9.07

Table 5: Kinetic parameters for the thermal decomposition of the compounds

Compound	Step	Coast - Redfern equation				Horowitz - Metzger equation			
		<u>r</u>	n	E	Z	<u>r</u>	n	E	Z
2	1 st	0.9993	0.00	43.7	8.81 x 10 ²	0.9995	0.00	47.1	3.38 x 10 ⁵
		0.9998	0.33	53.2	10.70 x 10 ²	0.9997	0.33	55.5	3.72 x 10 ⁴
		0.9999	0.50	58.4	11.74 x 10 ²	0.9998	0.50	60.1	3.15 x 10 ⁵
		0.9999	0.66	64.1	12.88 x 10 ²	0.9999	0.66	64.4	3.03 x 10 ⁵
		1.0000	1.00	76.0	15.28 x 10 ²	1.0000	1.00	75.0	7.28 x 10 ⁵
		0.9998	2.00	118.8	24.14 x 10 ²	0.9998	2.00	111.9	11.10 x 10 ⁵
3	1 st	0.9993	0.00	35.6	7.19 x 10 ²	0.9994	0.00	47.0	7.64 x 10 ³
		0.9998	0.33	46.1	9.29 x 10 ²	0.9998	0.33	58.0	1.16 x 10 ²
		0.9999	0.50	52.3	10.53 x 10 ²	0.9999	0.50	64.2	3.63 x 10 ²
		1.0000	0.66	58.9	11.85 x 10 ²	1.0000	0.66	70.7	6.47 x 10 ²
		1.0000	1.00	73.6	14.78 x 10 ²	1.0000	1.00	85.5	3.68 x 10 ³
		0.9994	2.00	128.3	26.06 x 10 ²	0.9995	2.00	141.8	8.17 x 10 ⁶

E in kJ mol⁻¹, underlined *r* in all tables represents the best fit values of n and E

Table 6: Thermodynamic parameters for the thermal decomposition of the compounds

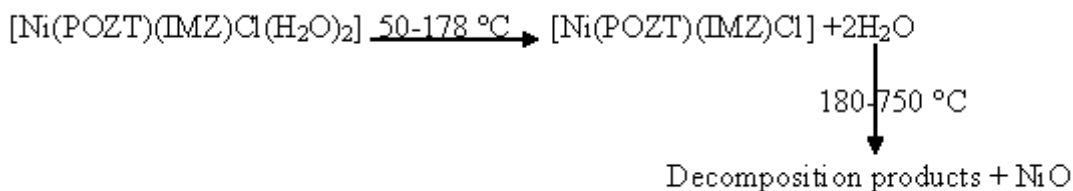
Compound	Step	ΔS*	ΔH*	ΔG*
2	1 st	-194.19	38.79	114.61
3	1 st	-196.62	30.24	126.65

ΔH*, ΔG* are in kJ mol⁻¹ and ΔS* in kJ mol⁻¹ K⁻¹

Thermal Studies

The TG and DTG data are presented in Table (4). The thermal decomposition of the coordination polymers has been investigated in dynamic air from ambient temperature to 750 °C. As typical example the thermogram of the Ni(II)

compound **2** in dynamic air shows four steps in the temperature ranges 50-178, 180-370, 372-453 and 455-750 °C (Fig.4). The first step corresponds to the release of the two coordinated water molecules (calc.9.57 %, found 8.53 %). The DTG curve show this step at 156 °C and an endothermic peak appears at 160 °C in the DTA trace. The second, third and forth steps represent a loss of weight indicating the decomposition the ligands. This steps appear in the DTG curve at 315, 405 and 480 °C and are associated with exothermic peaks at 317, 407 and 482 °C in the DTA curve. The final product was identified on the basis of mass loss considerations to be NiO as the residual part (calc. 19.83 %, found 20.64 %) (Scheme 1).



Kinetic analysis

Non-isothermal kinetic analysis of the complexes was carried out applying two different

procedures: the Coats-Redfern²² and the Horowitz-Metzger²³ methods.

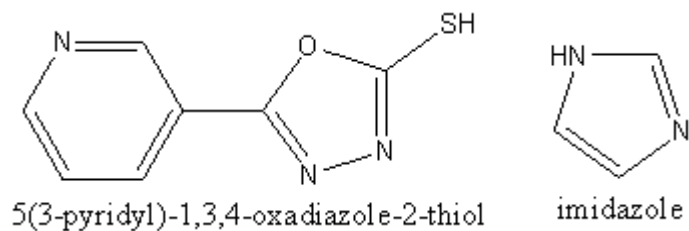


Fig. 1: Chemical structure of POZT and IMZ ligands

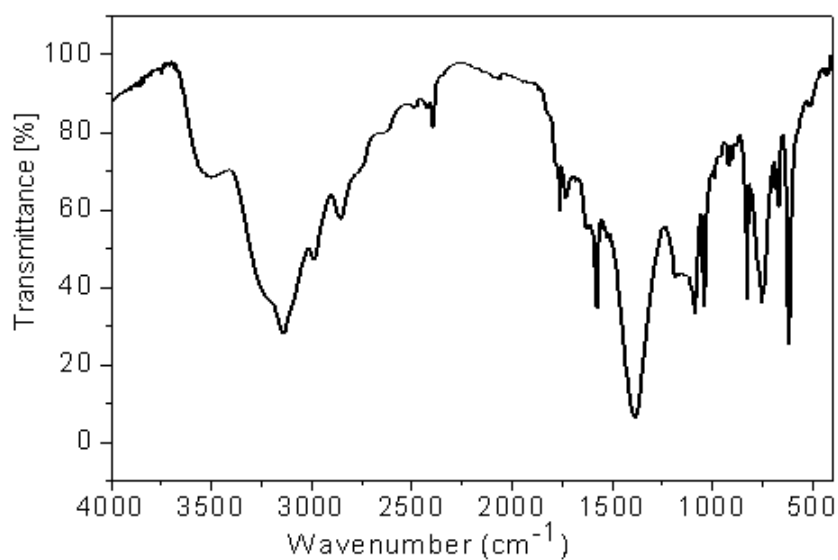


Fig. 2: FT-IR of compound 4

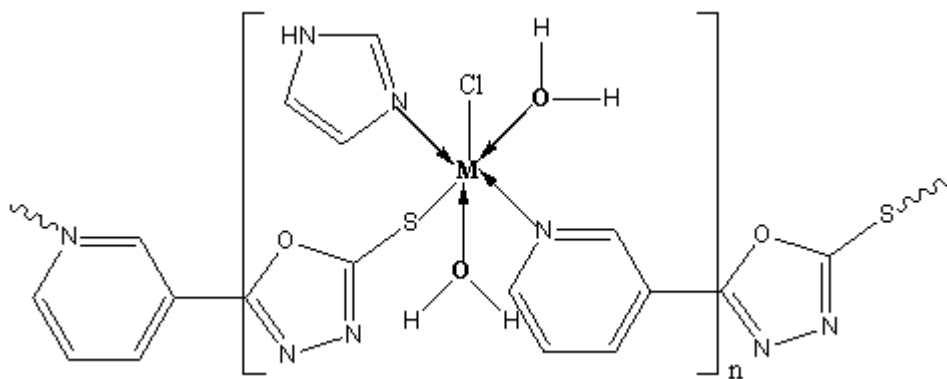


Fig. 3(a): Structure of $[M(\text{POZT})(\text{IMZ})\text{Cl}(\text{H}_2\text{O})_2]_n$ M = Co(II), Ni(II) and Cd(II)

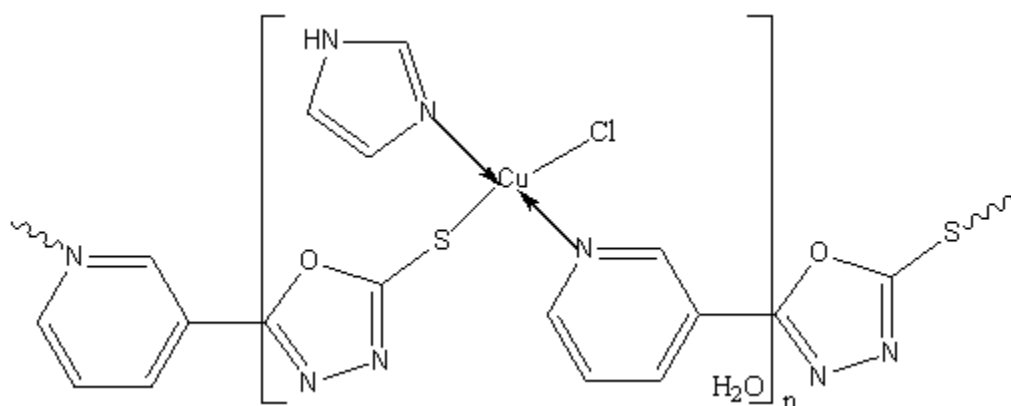


Fig. 3(b): Structure of $\{[\text{Cu}(\text{POZT})(\text{IMZ})\text{Cl}]\cdot\text{H}_2\text{O}\}_n$

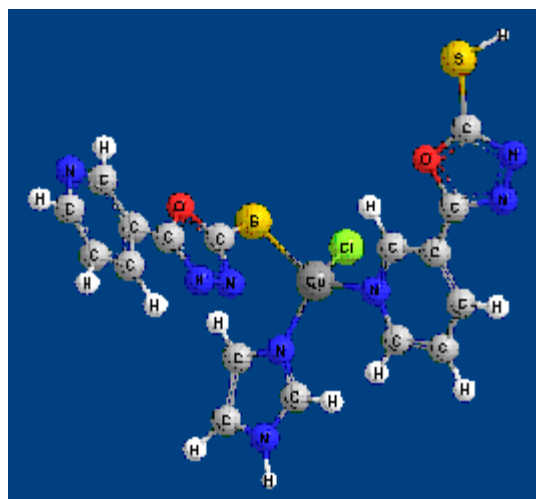


Fig. 3(c): A perspective view of the coordination around Cu (II)

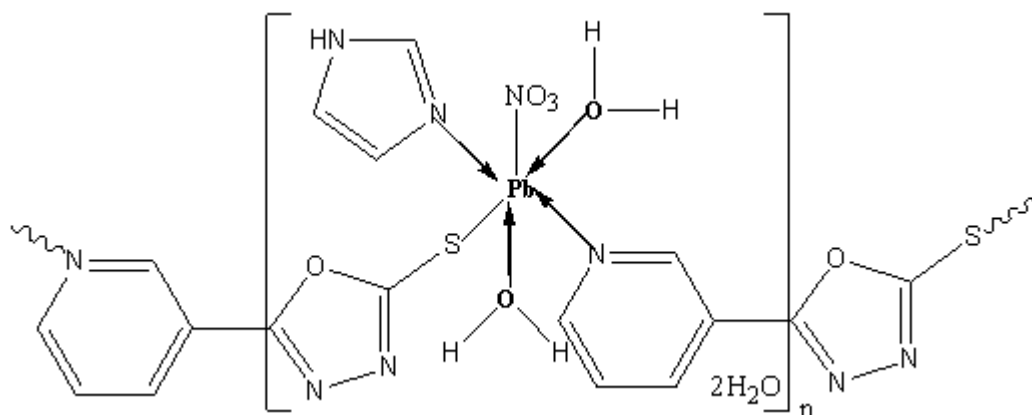


Fig. 3(d): Structure of $\{[\text{Pb}(\text{POZT})(\text{IMZ})(\text{NO}_3)(\text{H}_2\text{O})_2]\cdot 2\text{H}_2\text{O}\}_n$

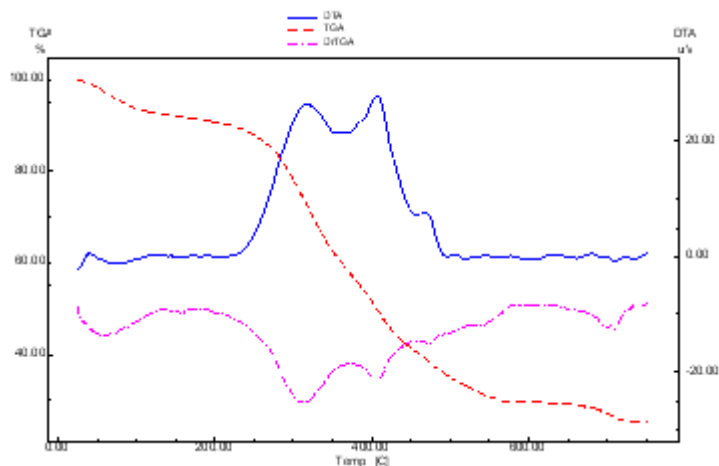


Fig. 4: TG, DTG and DTA thermograms of compound 2 in dynamic air

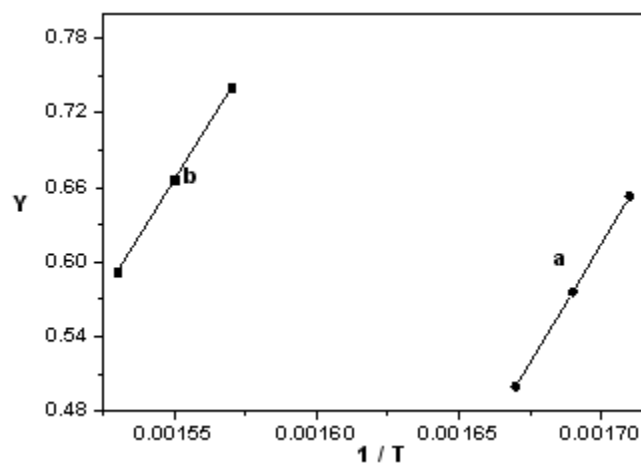


Fig. 5: Coats-Redfern plots for a) compound 2 and b) compound 3 first step in dynamic air where $Y = \ln[1 - (1 - \alpha)^{1-n}] / (1 - \alpha) T^2$ for $n \neq 1$ or $Y = \ln[-\ln(1 - \alpha) / T^2]$ for $n = 1$

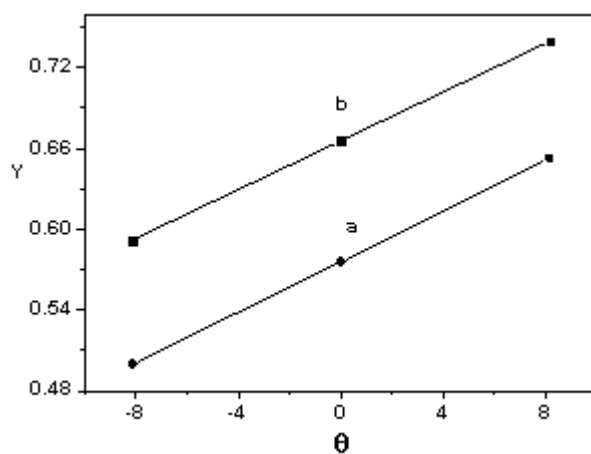


Fig. 6: Horowitz-Metzger plots for a) compound 2 and b) compound 3 first step in dynamic air where $Y = \ln[1 - (1 - \alpha)^{1-n}] / (1 - n)$ for $n \neq 1$ or $Y = \ln[-\ln(1 - \alpha)]$ for $n = 1$

Table 7: Microbiological screening of the compounds

Comp.	<i>B. cereus</i> (G+ve)	<i>S. aureus</i> (G+ve)	<i>S. marcescens</i> (G+ve)	<i>E. coli</i> (G+ve)	<i>P. aeruginosa</i> (G+ve)	<i>A. flavus</i> (G+ve)	<i>C. albicans</i> (G+ve)	<i>F. oxysporum</i> (G+ve)	<i>T. rubrum</i> (G+ve)	<i>G. candidum</i> (G+ve)	<i>S. brevicaulis</i> (G+ve)
1	16	14	13	12	12	0	0	0	12	10	0
4	16	15	16	18	16	24	14	12	28	16	16
5	14	12	14	13	14	18	0	12	13	12	12

The Coats-Redfern equation

$$\ln[1-(1-\alpha)^{1-n}/(1-n)T^2] = M/T + B \text{ for } n \neq 1 \quad \dots(1)$$

$$\ln[-\ln(1-\alpha)/T^2] = M/T + B \text{ for } n = 1 \quad \dots(2)$$

where α is the fraction of material decomposed, n is the order of the decomposition reaction and $M = -E/R$ and $B = ZR/\Phi E$; E , R , Z and Φ are the activation energy, gas constant, pre-exponential factor and heating rate, respectively. The Horowitz-Metzger equation

$$\ln[1-(1-\alpha)^{1-n}/1-n] = \ln ZRT_s^2/\Phi E - E/RT_s + E\theta/RT_s^2 \text{ for } n \neq 1 \quad \dots(3)$$

$$\ln[-\ln(1-\alpha)] = E\theta/RT_s^2 \text{ for } n = 1 \quad \dots(4)$$

where $\theta = T - T_s$, T_s is the temperature at the DTG peak. The correlation coefficient r is computed using the least squares method for equations (1), (2), (3) and (4). Linear curves were drawn for different values of n ranging from 0 to 2. The value of n , which gave the best fit, was chosen as the order parameter for the decomposition stage of interest. The kinetic parameters were calculated from the plots of the left hand side of equations (1), (2), against $1/T$ and against θ for equations (3) and (4) (Figs.5 and 6). The kinetic parameters for compounds 2 and 3 are calculated for the first step according to the above two methods and are cited in Tables 5 and 6.

Negative ΔS^* values for the different stages of decomposition of the complexes 2 and 3 suggest that the activated complex is more ordered than the reactants and that the reactions are slower than normal²⁴⁻²⁶. The more ordered nature may be due to the polarization of bonds in the activated state, which

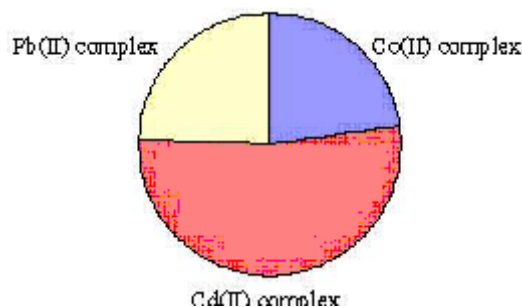


Fig. 11: Comparison of coordination polymers against *T. rubrum* fungi

might happen through charge transfer electronic transition²⁷. The different values of ΔH^* and ΔG^* of the complexes 2 and 3 refer to the effect of the structure of the metal ions on the thermal stability of the complexes²⁸. The positive values of ΔG^* indicate that the decomposition reaction is not spontaneous. Scanning Electron Micrographs (SEM) The scanning electron micrographs of cobalt(II) mixed ligand coordination polymer as representatives are given in Fig. 7.

Biological activity

In testing the antibacterial and antifungal activity of the compounds 1, 4 and 5 we used more than one test organism to increase the chance of detecting antibiotic principles in tested materials.

The data showed that in some cases the ligand has a higher or similar antimicrobial and antifungal activity than the selected standards (chloramphenicol and clotrimazole). Also, the complexes of certain metal ions enhanced the antimicrobial activity and in some cases a higher or similar activity than the selected standards were also shown (Table 7). Figures (8-11) show the antimicrobial effect for these compounds.

ACKNOWLEDGEMENTS

One of the authors (A. A. M. ALY) is very grateful to Alexander Von Humboldt Foundation for donating the magnetic susceptibility balance (MSB-Auto).

REFERENCES

1. B. Kesanli, W. Lin, *Coord. Chem. Rev.* **246**: 305 (2003).
2. N.L. Rosi, J. Kim, M. Eddaoudi, B. Chen, M. O'Keeffe, O.M. Yaghi, *J. Am. Chem. Soc.* **127**: 1504 (2005).
3. N.J. Melcer, G.D. Enright, J.A. Ripmeester, G.K.H. Shimizu, *Inorg. Chem.* **40**: 4641 (2001).
4. Q. Ye, Y.-H. Li, Y.-M. Song, X.-F. Huang, R.-G. Xiong, Z. Xue, *Inorg. Chem.* **44**: 3618 (2005).
5. P.D. Akrivos, *Coord. Chem. Rev.* **213**: 181 (2001).
6. M. Du, Z.-H. Zhang, X.-J. Zhao, Q. Xu, *Inorg. Chem.* **45**: 5785 (2006).
7. S.A. Barnett, N.R. Champness, *Coord. Chem. Rev.* **246**: 145 (2003).
8. S.J. Moore, R.J. Lachicotte, S.T. Sullivan, L.G. Marzilli, *Inorg. Chem.* **38**: 383 (1999).
9. E. Prenesti, S. Berto, P.G. Daniele, *Spectrochim. Acta A* **59**: 201 (2003).
10. E. Kim, K. Kamaraj, B. Galliker, N. Rubie, P. Loccoz, *Inorg. Chem.* **44**: 1238 (2005).
11. W. J. Geary, *Coord. Chem. Rev.* **7**: 81 (1971).
12. M. Singh, R. J. Butcher, N.K. Singh, *Polyhedron* **27**: 3151 (2008).
13. A. Das, C. Marschner, J. Cano, J. Baumgartner, J. Ribas, M. Salah and S. Mitra, *Polyhedron*. **28**: 2436 (2009).
14. T.K. Yazicilar and E.Y. Gurkan, *Transition. Met. Chem* **34**: 669 (2009).
15. A. Bravo and J. Anaconda, *Transition. Met. Chem.*, **26**: 20 (2001).
16. Y.T. Wang, G. M. Tang, W. Y Ma, W. Z. Wan, *Polyhedron* **26**: 782 (2007).
17. T. Rakha, *Synth. React. Inorg. Met.- Org. Chem.*, **30**: 205 (2000).
18. J. Kulhanek, F. Bures, T. Mikysek, J. Ludvik, O. Pytela, *Dyes and Pigments*, **90**: 48 (2011).
19. A. B. P. Lever, *Inorganic Electronic Spectroscopy*, 2nd Ed., Elsevier, Amsterdam, (1984).
20. D .X. West, J.P. Scovill, J.V. Silverton and A. Bavoso, *Transition Met. Chem.*, **11**: 123 (1986).
21. O. A. El-Gammal, *Mole. Biomole. Spec*, **75**: 533 (2010).
22. A. Coats and J. Redfern, *Nature.*, **20**: 68 (1964).
23. H. Horowitz and G. Metzger, *Anal. Chem.*, **35**: 1464 (1963).
24. Mohamed GG, Hosny WM, Abd El-Rahim MA. *Synthesis and React. in Inorg. and Met- Org. Chem.* **32**: 1501 (2000).
25. Beg MA, Qaiser MA. *Thermochimica Acta.* **210**: 123 (1998).
26. Pandey OP, Sengupta SK, Tripathi SC. A review *Thermochimica Acta*, **96**: 155 (1985).
27. Yusuff KM, Karthikeyan AR. *Thermochimica Acta.* **207**: 193 (1992).
28. Emam ME, Kanawy M, Hafe MH. *J. of Therm. Anal. and Calorim.* **63**: 75 (2001) .